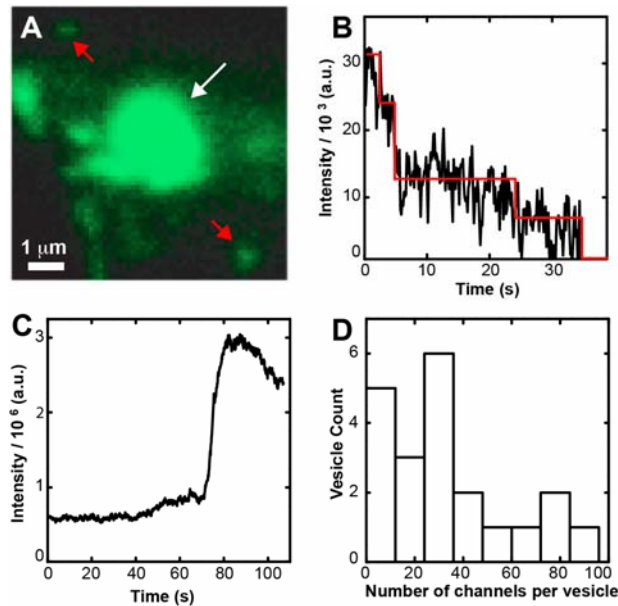
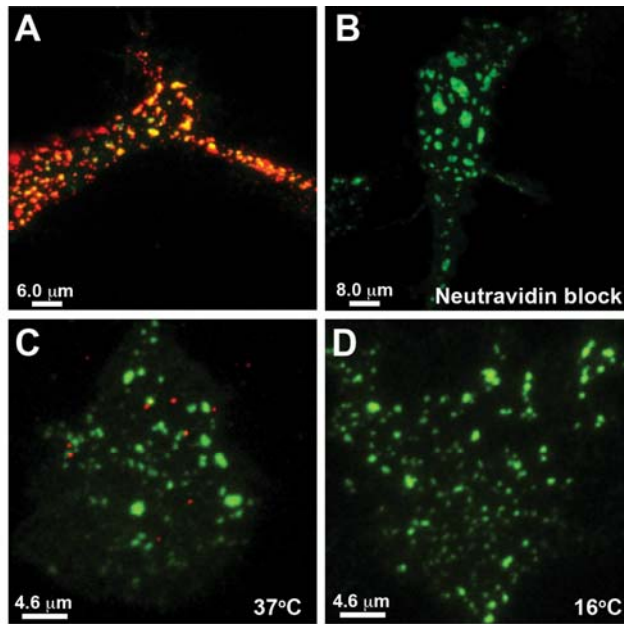


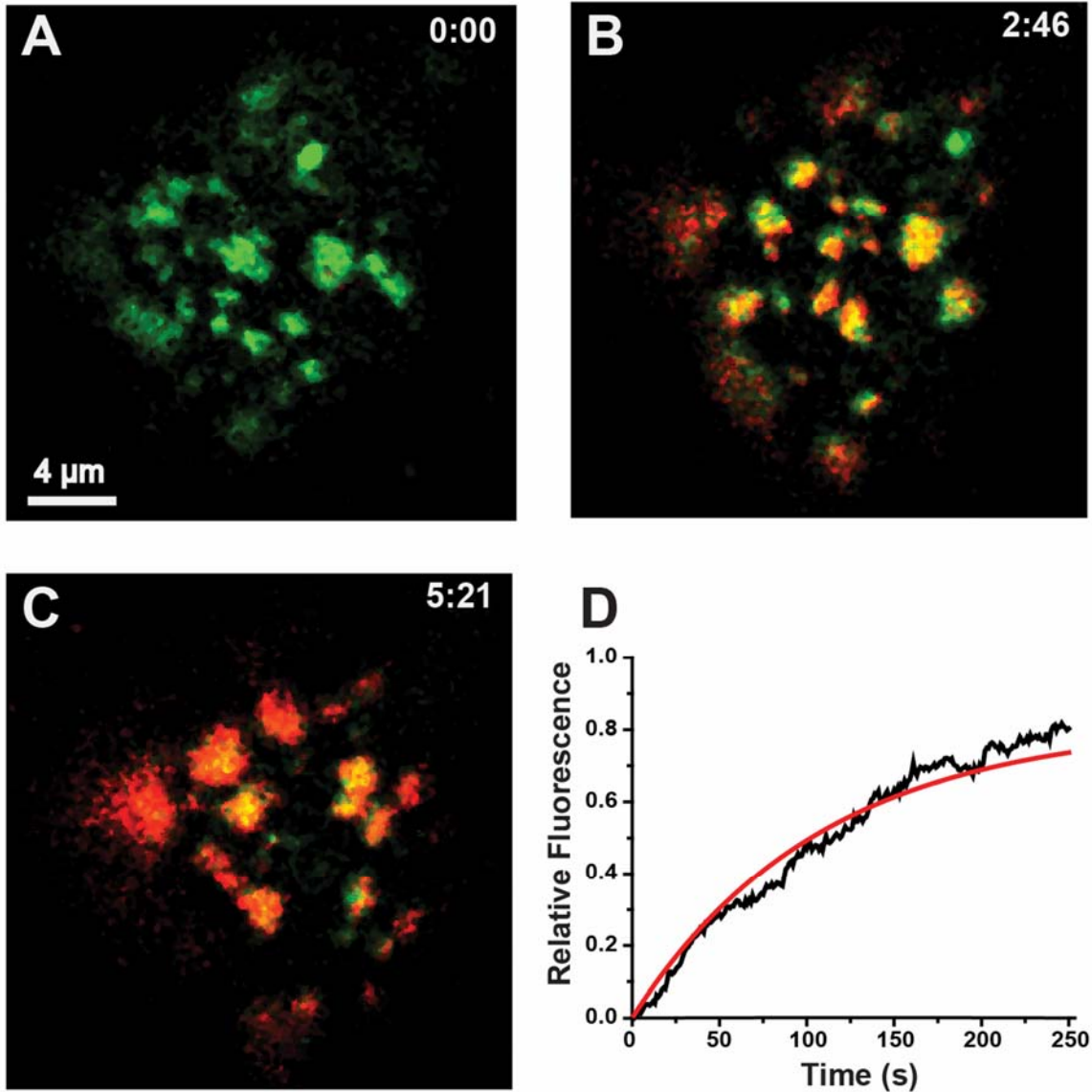
Supplementary figure legends



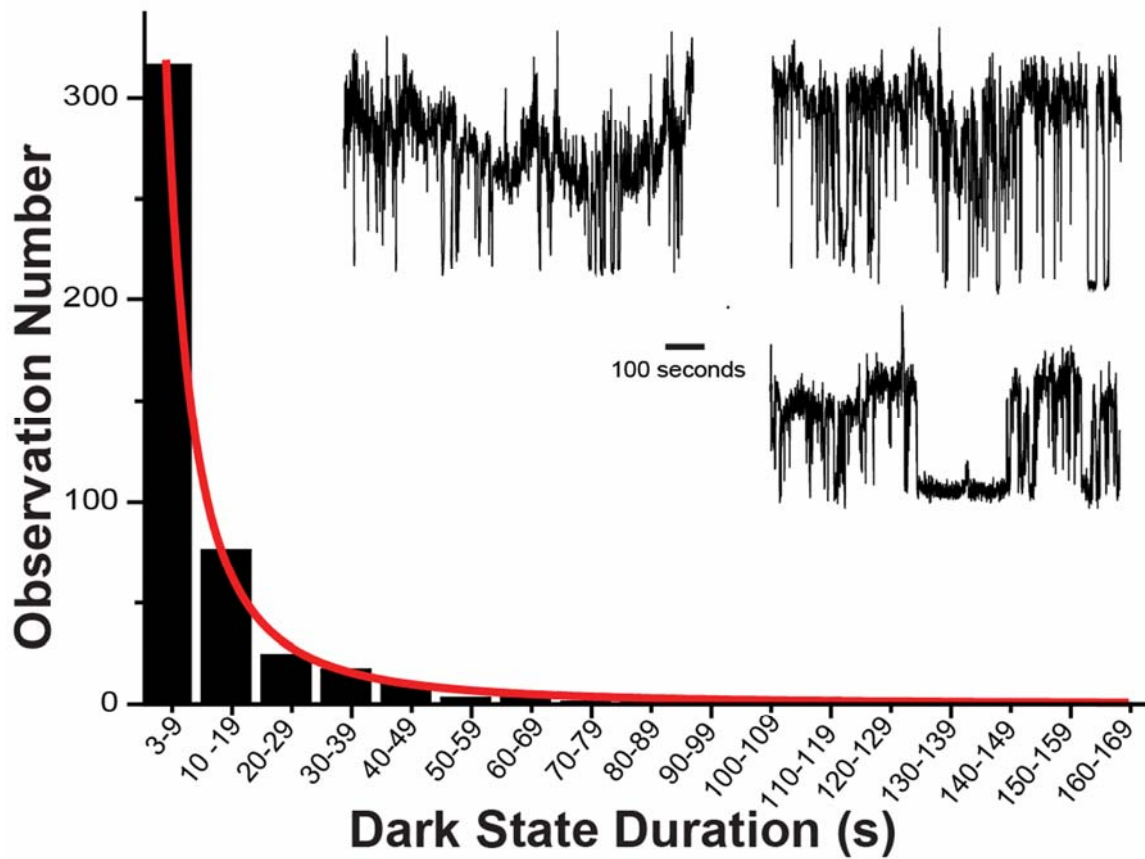
Supplementary Figure 1. Quantitation of Kv2.1 channel number in intracellular vesicles (A) Imaging of trafficking vesicles and single GFP-Kv2.1 channels. The red arrows indicate puncta defined as single Kv2.1 channels based on the number of photobleach states while the white arrow indicates a trafficking vesicle based on its rapid movement. (B) Representative four-step bleach within a single GFP-Kv2.1 channel during imaging at 8 Hz. The bleach step magnitude, illustrated by the red line, corresponds to the intensity of a single GFP. (C) Vesicle fluorescence reaches a maximum as it approaches the membrane. Fluorescence intensity is critically dependent on Z position in the TIR field. To relate vesicle fluorescence to that of single Kv2.1 channels in the plasma membrane peak vesicle intensity was obtained immediately prior to fusion and subsequent GFP-Kv2.1 delivery to the membrane as illustrated. (D) Number of GFP-Kv2.1 channels per trafficking vesicle. These values were determined from vesicle GFP intensity and single channel bleach step magnitude, assuming four GFP molecules per channel was assumed. The indicated error was derived from variability in the single GFP bleach steps. Single GFP was determined from 190 bleach steps in 10 cells.



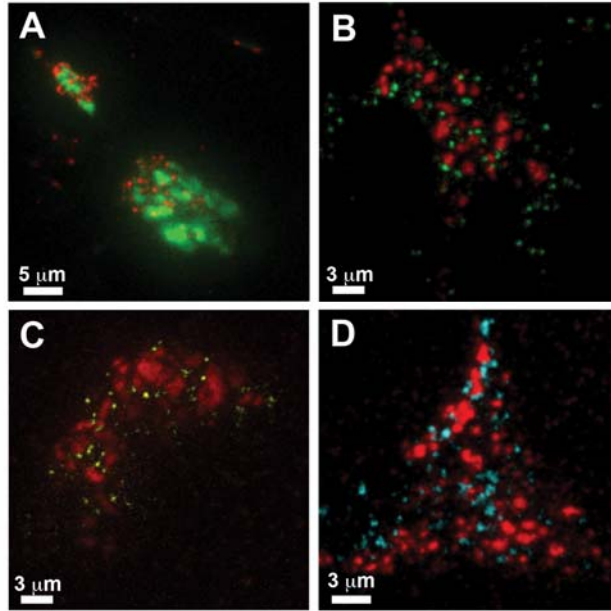
Supplementary Figure 2. Specificity of Qdot binding. (A) Qdot binding to HEK cells expressing biotinylated GFP-Kv2.1-loopBAD without neutravidin block. Cells were incubated with 1 nM 605 Qdots in imaging saline with 1% BSA for 10 min at 37°C, unbound Qdots then removed and the cell immediately imaged using TIRF optics. The red Qdot binding obscures the green GFP signal. (B) Qdot binding following neutravidin block. Cells were first incubated 1 μM neutravidin in imaging saline for 5 min at 37°C. Following neutravidin removal the cell were Qdot labeled as in A. (C and D) Surface delivery of Kv2.1 at 37 and 16°C, respectively. Qdot binding as in A was performed following neutravidin block and incubation at either 16 or 37°C for 45 min. Following the 37°C incubation 7 of 9 bound Qdots were cluster associated. One Qdot at 12 o'clock is obscured by the bright GFP cluster it is within and one Qdot at 4 o'clock is obscuring the small green cluster it colocalizes with. Overall, 89±9% of Qdots (n=211 from 14 cells) in this type of assay were cluster associated. The lack of any bound Qdots in panel D is expected since no insertion of Kv2.1 channel should occur at the 16°C temperature.



Supplementary Figure 3. Time course of Qdot binding to GFP-Kv2.1-loopBAD channels. (A-C) Qdot binding observed at the indicated times following the addition of a 1 nM Qdot solution. (D) Quantitation of Qdot fluorescence over time. The data from three binding time courses were normalized, averaged and fitted to $I = I_{\max} (1 - \exp^{-t/\tau})$. Here $\tau=108$ sec. Since $t_{50\%} = \tau(2)$, the fitted curve indicates binding reached 50% at 75 s.



Supplementary Figure 4. Qdot blinking behavior under the imaging conditions used. Nontransfected HEK cells were incubated with 0.1 nM 605 Qdots in imaging saline without BSA for 10 min at 37°C, washed and the non-specifically bound, immobile Qdots imaged at 2-10 Hz in TIRF to quantitate the duration of any long-lived dark states. The three traces shown illustrate the typical blinking behavior observed and the histogram summarizes data collected from 26 Qdots. Only 14 of 460 long-lived dark states exceeded 60 s during >22,000 sec of imaging. The histogram was fit with a power law, $N=27021t^{-2}$.



Supplementary Figure 5. Clathrin and caveolins prefer the Kv2.1 cluster perimeter.

(A) Relationship between RFP-clathrin light chain and GFP-Kv2.1 surface clusters in transfected 7DIV hippocampal neurons. In the 11 neurons examined, $76 \pm 15\%$ of the clathrin puncta were within $0.5 \mu\text{m}$ of the cluster perimeter while the perimeter occupied only $8 \pm 2\%$ of the basal cell surface. (B) Relationship between GFP-clathrin light chain and Kv2.1-HA surface clusters in transfected HEK cells. Kv2.1-HA was visualized using AlexaFluor594-conjugated anti-HA antibody. $60 \pm 9\%$ (9 cells) of the puncta were cluster-associated while the cluster perimeter occupied only $14 \pm 6\%$ of the basal cell surface. (C and D) Relationship between YFP-caveolin 1 or CFP-caveolin 3, respectively, and Kv2.1-HA surface clusters in transfected HEK cells. $66 \pm 10\%$ (9 cells) of the YFP-caveolin 1 puncta were within $0.5 \mu\text{m}$ of the Kv2.1 cluster perimeter while the perimeter occupied $16 \pm 5\%$ of the basal cell surface. $64 \pm 14\%$ (6 cells) of the CFP-caveolin 3 puncta were adjacent to the cluster while the perimeter occupied only $17 \pm 5\%$ of the basal cell surface.

Supplementary Table I

Qdot based detection of cytoplasmic Kv2.1 insertion into the plasma membrane of transfected HEK cells

Location of Qdot appearance based on manual detection

Cell #	QDots appearing within 0.5 μm of a cluster border	QDots appearing at cluster-free membrane	Percentage appearances associated with a cluster	% basal surface area in clusters
1	36	11	76.7	7.2
2	3	1	75	36.8
3	29	8	78.4	9.7
4	30	0	100	24.0
5	31	4	88.6	10.1
6	25	4	87.1	18.5
7	13	4	81	16.5
8	22	2	91	15.1
Total	189	34	84.7\pm8.4	17.2\pm9.5